Structure of Binary and Ternary Complexes of Zinc and Cobalt Carboxypeptidase A As Determined by X-ray Absorption Fine Structure†

Ke Zhang‡ and David S. Auld*,§

Biostructures Institute, University City Science Center and Department of Biochemistry and Biophysics, University of Pennsylvania, Philadelphia, Pennsylvania 19104, and Center for Biochemical and Biophysical Sciences and Medicine and Department of Pathology, Harvard Medical School and Brigham and Women's Hospital, 250 Longwood Avenue, Boston, Massachusetts 02115

Received August 4, 1995; Revised Manuscript Received October 2, 1995⊗

ABSTRACT: Carboxypeptidase A, ZnCPD, is typical of a wide range of exo- and endo-metalloproteases that have three protein ligands and a water molecule bound to a catalytic zinc atom and a glutamate residue in the active site that likely acts in conjunction with the Zn-bound water to bring about catalysis. Such enzymes generally have bell-shaped pH-activity profiles ($EH_2 \rightleftarrows EH \rightleftarrows E$) where the concentration of the catalytic species EH is regulated by pK_{EH_2} and pK_{EH}. The present X-ray absorption fine structure, XAFS, study has determined the structure and pH behavior of the binary and ternary product complexes in order to examine the role of the Zn-bound water in catalysis. Increasing the pH from 7 to 10 of the ZnCPD•L-Phe complex results in the same type of progressive spectral changes in the near-edge XAFS spectrum as is seen for ZnCPD, but the changes are complete by more than 1 pH value below that observed for ZnCPD. The results are in agreement with kinetic studies that show E binds the protonated form of L-Phe more tightly than EH, thus in effect decreasing the value of pK_{EH}. The XAFS results show the average interatomic distance, R, for the zinc ligands of the EH•L-Phe complex decreases by 0.02 Å upon formation of the E•L-Phe complex, essentially identical to that obtained for the EH and E forms of the native enzyme. Addition of azide to ZnCPD•L-Phe at pH 7 markedly changes the zinc coordination sphere from 4 N/O atoms at 2.021 ± 0.06 Å and 1.4 ± 0.5 N/O atoms at 2.54 ± 0.5 Å to 3.9 N/O atoms at 1.995 ± 0.006 Å. The decrease in R of about 0.03 Å in both the Zn- and CoCPD•L-Phe•N_3^- complexes is likely due to the ligand exchange from a neutral water to an anion. The XAFS spectra of the ternary complex is pH independent from 7 to 9, in agreement with the ionization of the water being the source of the spectral changes in the free enzyme and its binary L-Phe complex. The enzyme•azide•L-Phe complex is likely bound in a manner analogous to that expected for a post-transition state in a biproduct complex for peptide hydrolysis—that is, the carboxylate anion of the peptide bound to the Zn and the protonated form of L-Phe H-bonded to the catalytic Glu-270 carboxylate. The XAFS results on the "spectroscopically silent" ZnCPD are compared to nuclear magnetic resonance and electron absorption studies on CoCPD.

Carboxypeptidase A, ZnCPD,[1] is the standard of reference for a family of zinc exopeptidases having closely similar catalytic zinc sites based on alignments of their primary structure (Vallee & Auld, 1990a). It has a catalytic zinc bound to His-69 and Glu-72 at the ends of a reverse turn, His-196 supplied by a β sheet extending from residues 191 to 196 and a water molecule (Rees et al., 1983). We have recently begun to explore its mechanistic features by means of X-ray absorption fine structure, XAFS (Zhang et al., 1992, 1995; Zhang & Auld, 1993; Auld & Zhang, 1995).

The XAFS spectra of ZnCPD in solution progressively change, particularly in the near edge region, when the pH is changed from neutral to alkaline values (Zhang & Auld, 1993). Direct comparison of the first and higher coordination shells of ZnCPD reveals structural differences between pH 7 and 10 which are principally reflected in a decrease in the average inner coordination distance from 2.024 to 2.002 Å. Structural analyses of ZnCPD at intervening pH values show that this distance decreases as a function of the increase in pH. The XAFS Debye−Waller factor reveals increased structural disorder for the four-atom distribution at the alkaline pH value, while the higher shell comparison shows that the histidine ligands, His-69 and His-196, remain unchanged as the pH is increased. The pH-dependent decrease in the average interatomic distance and increased structural disorder is most easily explained by ionization of the metal-bound water. The plot of the normalized spectral differences between two peaks located near the absorption edge as a function of pH conforms to a theoretical pH-titration curve with a pK_a of 9.49 at −4 °C (Zhang & Auld, 1993). This value corresponds to that obtained by extrapolation of the temperature-dependent value of pK_{EH} obtained by kinetic analysis of the carboxypeptidase A−catalyzed hydrolysis of tripeptides to −4 °C (Auld & Vallee, 1970, 1971). The conversion of EH into E, regulated by pK_{EH}, leads to decreased catalysis due to weaker substrate binding. Thus the combined results of the XAFS and kinetic studies

† Supported by NIH Grant GM-47534.
* To whom correspondence should be addressed.
‡ University of Pennsylvania.
§ Harvard Medical School and Brigham and Women's Hospital.
⊗ Abstract published in *Advance ACS Abstracts,* November 15, 1995.
[1] Abbreviations: ZnCPD, native carboxypeptidase A; CoCPD, cobalt(II)-substituted carboxypeptidase A; RDF, radial distribution function; Im, imidazole; Ac, acetate; Mops, 3-(*N*-morpholino)propanesulfonic acid; Hepes, *N*-(2-hydroxyethyl)piperazine-*N*′-(2-ethanesulfonic acid); Ampso, 3-[(1,1-dimethyl-2-hydroxyethyl)amino]-2-hydroxypropanesulfonic acid; Ches, 2-(*N*-cyclohexylamino)ethanesulfonic acid.

0006-2960/95/0434-16306$09.00/0

indicate that the conversion of EH into E likely represents the ionization of the zinc-ligated water molecule in ZnCPD.

In the present investigation we have examined the coordination properties of the zinc and cobalt sites in binary product and ternary anion complexes. The results provide further evidence for the assignment of the alkaline pK_{EH} to ionization of the metal-bound water. This ionization strengthens the Zn−OH bond, requiring substrates and inhibitors to displace hydroxide instead of water.

MATERIALS AND METHODS

Enzyme Preparation. Bovine carboxypeptidase A was obtained from Sigma Chemical Co., St. Louis, MO (C-0261, lot no. 10H8040 and 10H8041). The commercial enzyme was purified by affinity chromatography and crystallization as previously described (Larsen & Auld, 1989; Zhang & Auld, 1993). The enzyme was stored as a crystalline suspension in deionized water at 4 °C. CoCPD was prepared from crystalline ZnCPD (Auld, 1988).

Preparation of Samples for XAFS. The aqueous phase of the crystalline enzyme suspension was removed by centrifugation in a microfuge, and the crystals were dissolved in a 1:1 volume ratio of 2 M NaCl, 20 mM Mops, pH 7.0. Further dilutions were made with buffered 1 M NaCl solutions. The protein concentration was always in the range 1.6 to 2.4 mM for the XAFS measurements. The L-phenylalanine (L-Phe) and sodium azide concentrations were 24 mM and 100 mM, respectively. These concentrations ensure 96−100% conversion of the free enzyme into the inhibitor complex based on kinetic studies of the zinc enzyme (Auld & Vallee, 1987) and spectral studies of the cobalt enzyme (Bicknell et al., 1988). Solid samples of $Zn(Im)_2(Ac)_2$ and $Co(Im)_2(Ac)_2$ were prepared by casting a fine crystalline powder (400 mesh) on a piece of Scotch tape.

All stock buffer and salt solutions were extracted with 0.02% dithizone in CCl_4 (Fisher 99 mol %) to remove metals (Holmquist, 1988). Deionized water was used in all dilutions. The buffers used to control pH were usually close to their pK_a values: Mops (pK_a, 7.10), Hepes (pK_a, 7.5), Ampso (pK_a, 9.00), and Ches (pK_a, 9.25). The buffer concentration in the XAFS samples was usually 100−110 mM.

XAFS Measurements. XAFS experiments were conducted at the Biostructures PRT beam line X9-A of the National Synchrotron Light Source of Brookhaven National Laboratory. A double-crystal, constant-exit-height monochromator and a Ni-coated Al harmonic rejection mirror were used for the measurements. The Si(220) crystal monochromator was used for all the measurements to ensure a good energy resolution, except for the full XAFS spectra collected on ZnCPD·L-Phe·N_3^- at pH 7, where a Si(111) crystal monochromator was used. The XAFS measurements were performed at 150 K using a closed cycle Displex helium refrigerator that controlled sample temperature to ≤1 degree K. A copper sample holder with Mylar windows was used for the XAFS measurements.

Several million effective photon counts were collected for each sample to ensure a good signal-to-noise ratio. The Zn and Co fluorescence of the sample after absorption of X-ray photons was collected using an energy-resolving 13-element Ge detector (Canbarra GL0110). The dead time of the detector system was calibrated on line for a wide range of incident count rates on each sample, corrected by approximation of the paralyzable model (Zhang et al., 1993). The incident count rate is maintained close to 50% of the saturation level for all individual detector elements.

pH Measurements. A Corning pH meter was standardized with pH 7 and 4 buffers at the indicated temperatures. The value of the pH 10 buffer was within 0.05 of its expected value. The pH values of all the samples were measured at 0 and 25 °C with a Calomel combination pH microelectrode (Aldridge Z11341-7) immediately before and after XAFS measurements. The change in pH was always less than 0.1 unit. The pH values quoted at −4 °C are extrapolated values based on the change in pH between 0 and 25 °C. Neither protein precipitation nor progressive spectral changes were observed during XAFS measurements.

Data Analysis. The XAFS $\chi(k)$ function was derived by subtraction of an atomic background, normalization to a constant edge step, and conversion of energy to electron wave-number k following the procedures previously outlined (Zhang et al., 1992; Zhang & Auld, 1993).

Quantitative data analysis of the first coordination shell was conducted by back-transforming the first shell distribution to k-space with a window function (Stern & Heald, 1983). A complex metal ion with similar metal coordination properties was required to model the enzyme-inhibitor metal binding site. Our previous studies have shown $Zn(Im)_2(Ac)_2$ and $Co(Im)_2(Ac)_2$ (Horrocks et al., 1980) to be excellent metal complexes for modeling the first coordination shell of Zn- and CoCPD (Zhang et al., 1992). The XAFS spectra of these compounds were reduced, transformed, and back-transformed in the same manner as was done for the proteins.

Both the radial distribution function (RDF) and the least-squares fitting method were used to analyze the XAFS data. The RDF method has been used previously for XAFS data analysis (Zhang et al., 1992; Zhang & Auld, 1993) and is complementary to the least-squares fitting method since it depends less on a preassumed structural model (Crozier et al., 1988; Stern et al., 1992). The RDFs were generated by 3 steps: removal of the central and backscattering phase shift and back scattering amplitude using the reference complex metal ion; cumulant expansion to extrapolate the data to $k = 0$; and Fourier sine transformation of the data that contain the structural information needed to construct the RDF.

The data were also analyzed by the least-squares fitting method to verify the RDF results, as previously described (Zhang et al., 1992, Zhang & Auld, 1993). The one- and two-distance distribution fits of the results were made using the reference metal ion complexes, $Zn(Im)_2(Ac)_2$ and $Co(Im)_2(Ac)_2$, and varying the coordination numbers, interatomic distances, and Debye−Waller factors. The quality of a fit, Q, was determined by an expression that takes into account the variation of error in k-space and the degrees of freedom in the data range (Zhang et al., 1988). The data range used for the fit is from 2 to 10 $Å^{-1}$, which gives about 7 degrees of freedom with a R-space window of 1.4 Å used in the back-transform (Lee et al., 1981).

RESULTS

The near-edge region of the X-ray absorption spectrum is sensitive to changes in the coordination properties of the metal. As a consequence, it can serve to titrate the effect of perturbants on the metal coordination sphere. Thus the change in the amplitude ratio of two near-edge peaks of

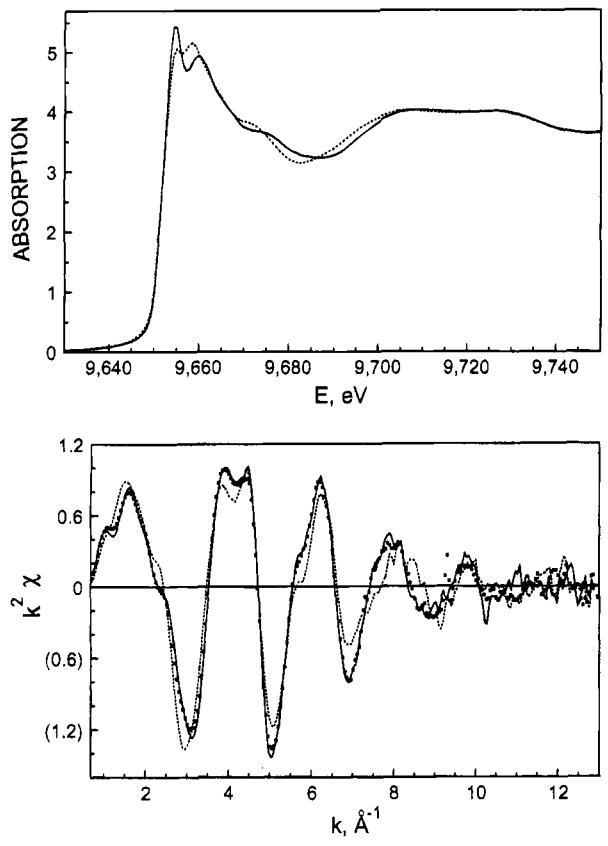

FIGURE 1: (A) Zn K-edge X-ray absorption near-edge spectra at 150 K for ZnCPD·L-Phe in 0.63 M NaCl, 24 mM L-Phe, 110 mM Mops, pH 6.56 at 25 °C (solid line) and 0.63 M NaCl, 24 mM L-Phe, 110 mM Ches, pH 8.83 at 25 °C (dashed line) and (B) their corresponding XAFS $\chi(k)$ function weighted by a k^2 factor. The XAFS $\chi(k)$ data for ZnCPD in 0.95 M NaCl, 50 mM Mops, pH 7.0 at 25 °C (squares) is given as a reference.

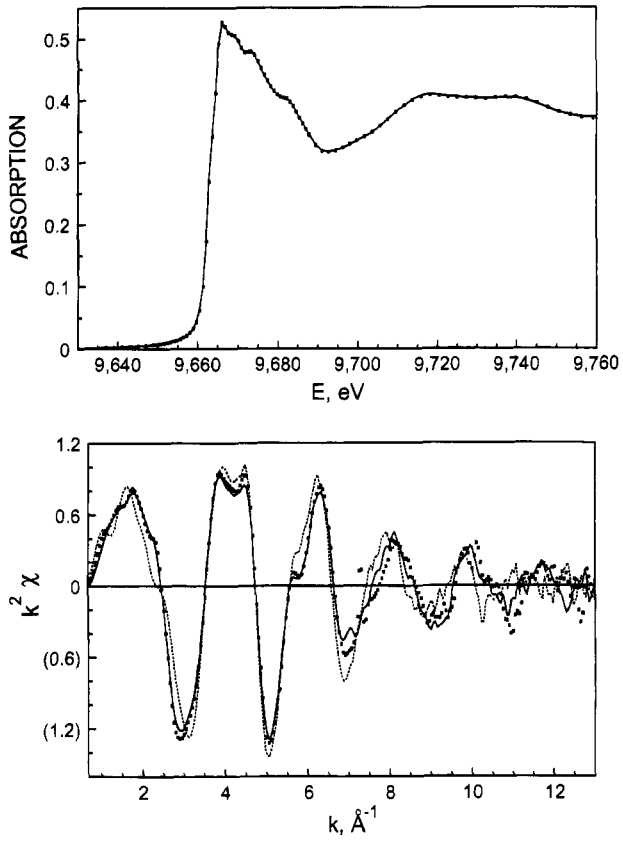

FIGURE 2: (A) Zn K-edge X-ray absorption near-edge spectra at 150 K for ZnCPD·L-Phe·N_3^- in 0.75 M NaCl, 24 mM L-Phe, 100 mM NaN_3, 50 mM Mops, pH 7.0 at 25 °C (solid line) and in 0.65 M NaCl, 24 mM L-Phe, 105 mM NaN_3, 105 mM Ampso, pH 8.81 at 25 °C (squares) and (B) their corresponding XAFS $\chi(k)$ function weighted by a k^2 factor. The XAFS $\chi(k)$ data for ZnCPD·L-Phe at pH 6.56 (dashed line) is given as a reference.

native ZnCPD as a function of pH can be described by the conversion of an EH form of the enzyme into an E form with a pK_a of 9.0 at 25 °C (Zhang & Auld, 1993). The L-Phe complex of ZnCPD at pH 6.56 and 25 °C has a near-edge spectrum and $\chi(k)$ function closely similar to that of the native enzyme at pH 7.0 (Figure 1, A and B). At pH 8.83 the ZnCPD·L-Phe complex has the same near-edge spectrum (Figure 1A) as seen for the native enzyme at a pH value one unit higher, 9.9 (Zhang & Auld, 1993). No further changes in the spectrum are observed for ZnCPD·L-Phe if the pH is increased to 10 (data not shown).

Addition of azide to the ZnCPD·L-Phe complex at pH 7 markedly changes the near-edge spectrum (Figures 1A and 2A) and the corresponding $\chi(k)$ function of the L-Phe complex at pH 6.56 (Figure 2B). The spectral changes are very different from those seen by pH titration of ZnCPD or its L-Phe complex (Figure 1). Increasing the pH of the ZnCPD·L-Phe·N_3^- complex to 8.81 does not produce any further change in the spectrum. Azide binding thus prevents the effect of pH seen for both the free enzyme (Zhang & Auld, 1993) and its L-Phe complex (Figures 1 and 2). The spectral changes accompanying the conversion of CoCPD·L-Phe into the CoCPD·L-Phe·N_3^- complex are similar to those observed for their respective zinc complexes (data not shown).

Fourier transforms of the $\chi(k)$ function generate pseudo radial distributions of atoms about the metal ion. The Fourier transforms of the ZnCPD·L-Phe and ZnCPD·L-Phe·N_3^-

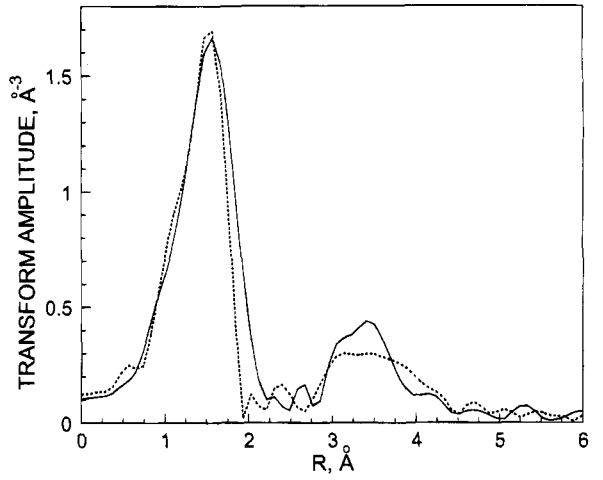

FIGURE 3: Fourier transform amplitudes of $k^2\chi(k)$ data of ZnCPD·L-Phe (solid line) and ZnCPD·L-Phe·N_3^- (dashed line) at neutral pH values. The transforms were performed between 1.0 and 12.5 Å^{-1} in k-space. The first coordination shell contribution was isolated using an R-space window of 0.7−2.2 Å.

complexes differ markedly at neutral pH values (Figure 3). The first shell peak of ZnCPD·L-Phe (located at 1.5 Å) moves to a slightly lower distance for ZnCPD·L-Phe·N_3^-, indicating structural changes in the first coordination shell of the metal ion. In addition, changes are observed for the higher shell distribution located between 3 and 4 Å in the region where a bound azide might be expected to affect the XAFS results.

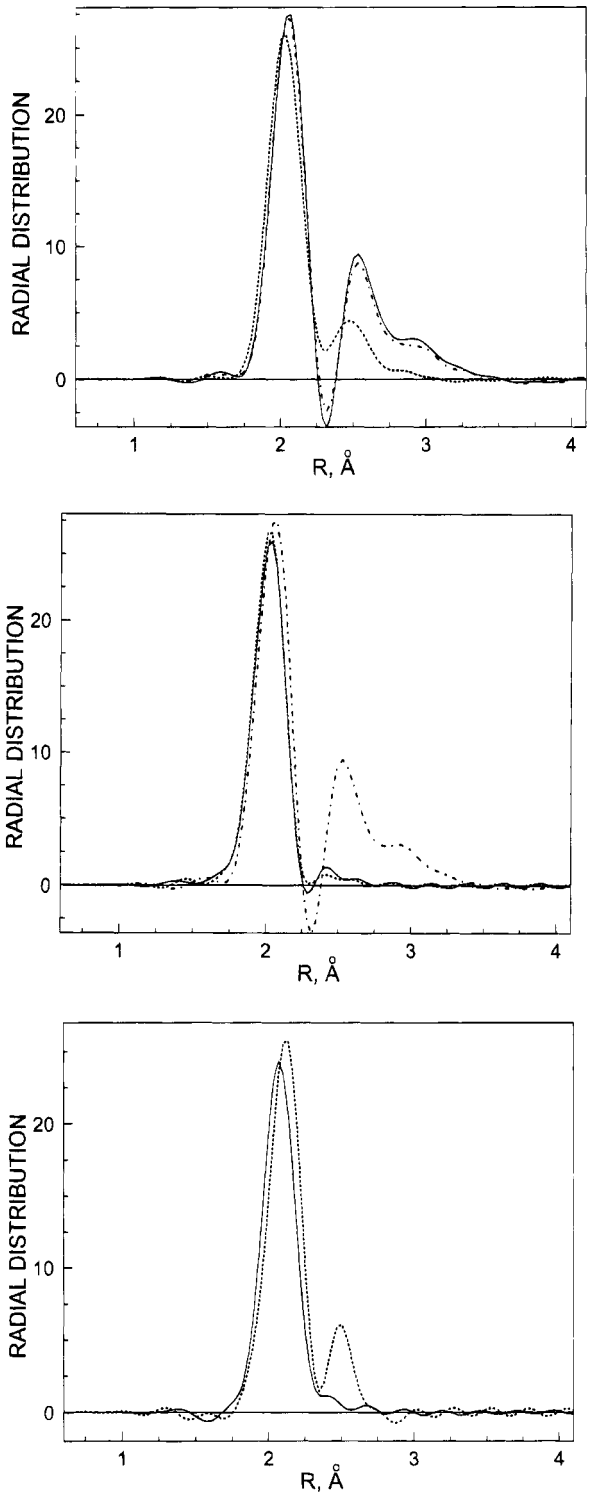

FIGURE 4: (A) The RDFs of ZnCPD·L-Phe at pH 6.56 (solid line) and 8.83 (dashed line) are compared to that of ZnCPD (dash dot line) at pH 7.0 all at 25 °C. (B) The RDF of ZnCPD·L-Phe·N_3^- at pH 7.0 (solid line) and 8.81 (dashed line) are compared to that of ZnCPD·L-Phe (dash-dot line) at pH 6.56. (C) The RDFs of CoCPD·L-Phe·N_3^- (solid line) and CoCPD (dashed line) both at pH 7.0. The RDFs were artificially broadened by a Gaussian factor $\sigma^2 = 0.01$ Å^2 to reduce the truncation effects. The metal ion complexes Zn- and $Co(IM)_2(Ac)_2$ are used for deriving the RDFs.

The RDFs of ZnCPD·L-Phe at pH values of 6.56 and 8.83 are compared to the RDF of the free enzyme at neutral pH in Figure 4A. The RDF of the metal ion complex, $Zn(Im)_2(Ac)_2$, generated according to its known structure (Horrocks et al., 1980), provides a quantitative reference (data not shown). The first shell RDF of ZnCPD·L-Phe at pH 6.56 is essentially the same as that of the free enzyme at neutrality. Both contain two atomic distributions. At pH 6.56, the larger distribution of the ZnCPD·L-Phe complex and ZnCPD has 4 ligand atoms (oxygen or nitrogen) located at 2.020 Å from the metal atom, and the smaller distribution has 1.3 atoms located at 2.56 Å from the metal atom. At pH 9.0 the four-atom distribution of the ZnCPD·L-Phe complex changes to a shorter distance of 2.001 Å, and the smaller distribution reduces to 0.7 atom located at 2.46 Å. The pH-dependent change of this distribution is essentially identical to that observed for the free enzyme over the pH range 7 to 10 (Zhang & Auld, 1993).

Table 1: Structural Parameters for the Catalytic Metal of Zn- and CoCPD and Their Inhibitor Complexes[a]

enzyme	N[b]	R[c] (Å)	σ^2 [d] (Å^2)	N[b]	R[c] (Å)	σ^2 [d] (Å^2)	Q[e]
ZnCPD[f] pH 7.0 (7.2)	4	2.024(6)	−0.001	1.3(4)	2.54(5)	−0.0012	1.0
ZnCPD·L-Phe pH 6.56 (6.94)	4	2.021(6)	0.000	1.4(5)	2.54(5)	−0.002	1.0
ZnCPD·L-Phe pH 7.99 (8.38)	4	2.012(6)	0.001	0.9(5)	2.49(5)	0.001	0.9
ZnCPD·L-Phe pH 8.57 (9.25)	4	2.002(6)	0.001	0.8(4)	2.47(5)	0.002	0.4
ZnCPD·L-Phe pH 8.83 (9.55)	4	2.001(6)	0.001	0.7(4)	2.47(5)	0.001	0.4
ZnCPD·L-Phe·N_3^- pH 7.0 (7.2)	3.9(5)	1.995(6)	0.000				0.7
ZnCPD·L-Phe·N_3^- pH 8.81 (9.36)	4.0(5)	1.995(6)	0.000				0.6
CoCPD[g] pH 7.0 (7.2)	4	2.08(1)	0.002	1.0	2.50(4)	0.000	0.6
CoCPD·L-Phe·N_3^- pH 7.0 (7.2)	4.1(5)	2.046(7)	0.001				0.6

[a] First shell fitting results using the least-squares method of analysis described previously (Zhang et al., 1992). The pH values given in parentheses are those of the solution at its freezing point, −4 °C. [b] Zinc coordination number. [c] Average absorber−scatterer bond lengths. [d] Mean-square deviation in absorber−scatterer in angstroms squared. [e] Fitting criteria (Zhang et al., 1988). [f] Results from Zhang and Auld (1993). [g] Results from Zhang et al. (1992).

The RDFs of the ZnCPD·L-Phe·N_3^- complex at pH values of 7.0 and 8.81 are compared with the RDF of the ZnCPD·L-Phe complex at pH 6.56 (Figure 4B). The RDF of ZnCPD·L-Phe·N_3^- at pH 7 is essentially the same as that at pH 8.81. In both cases four ligand atoms are located at 1.993 Å from the zinc atom. This represents a substantial structural change from that observed for the ZnCPD·L-Phe complex or the free enzyme (Figure 4A). Thus the four-atom distribution located at an average distance of 2.024 Å in ZnCPD is shortened by 0.031 Å, and the smaller distribution located at 2.5−2.6 Å completely disappears. The differences in the RDFs of CoCPD and CoCPD·L-Phe·N_3^- are similar to those observed for the zinc species (Figure 4C). The four-atom distribution in the first shell of CoCPD·L-Phe·N_3^- is located at 2.044 Å, a 0.036 Å reduction from that for the free enzyme (Zhang et al., 1992) and the second distribution of one atom at ~2.5 Å again disappears.

Least-squares fitting analyses of the data yield R values that are nearly identical to those obtained from RDF analyses. The results of the best fit for which the Q values are smaller or equal to unity are listed in Table 1. Satisfactory fits with Q less than 1 cannot be obtained for ZnCPD·L-Phe at pH 7.2 using a single distance distribution of atoms, while good fits are obtained for the ternary complexes ZnCPD·L-Phe·N_3^-

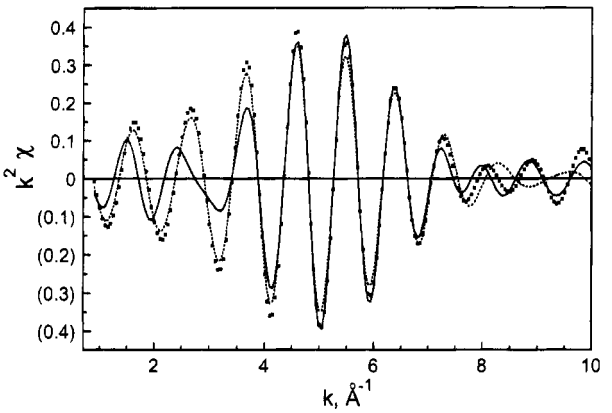

FIGURE 5: Zn K-edge XAFS χ data of the higher coordination shell of ZnCPD·L-Phe·N_3^- (solid line) isolated from 2.8 to 4.0 Å in the Fourier transform (Figure 3) compared with the χ data of ZnCPD (dashed line) and ZnCPD·L-Phe (squares). The data are weighted by a k^2 factor.

and CoCPD·L-Phe·N_3^- using a single distance model. A mathematical model employing two distributions of atoms with different distances does not improve the quality of the fit for the ternary complexes of either the Zn or Co enzyme. In addition, this model yields an unreasonably large Debye–Waller factor for the smaller atom distribution. Thus the first shell fit using the two-distance model for ZnCPD·L-Phe·N_3^- obtained the same four-ligand atom distribution and a single ligand atom distributed with a Debye–Waller factor of 0.12 Å^2. Such a large Debye–Waller factor diminishes the contribution of the single atom, in effect making the analysis a one-distance, four-ligand atom distribution and indicating that the presumed two-distance distribution is unrealistic.

The average interatomic distance, R, for the ZnCPD·L-Phe complex decreases as the pH increases from 6.56 to 8.83 (Table 1). The total change in interatomic distance, 0.020 Å, is nearly identical to that observed for the native enzyme, 0.022 Å, over the pH range 7 to 9.9 (Zhang and Auld, 1993). Thus the pH related decrease in this distance occurs for both the free enzyme and its L-Phe product complex.

The higher shell contributions to the XAFS spectrum located between 2.8 and 4.0 Å in the Fourier transforms (Figure 3) are isolated and back transformed for ZnCPD·L-Phe·N_3^- and ZnCPD·L-Phe (Figure 5). This Fourier transform peak is mainly due to the C-4 carbons and N-3 nitrogens of the histidines that are colinear with N1, the zinc ligand, and thus enhanced by the focusing effect (Bunker et al., 1982). However, multiple scattering contributions having similar path lengths also largely affect this peak at the low k (below 3 Å^{-1}) region (Zhang & Auld, 1993). Qualitative comparisons of the $\chi(k)$ function can be made between ZnCPD·L-Phe·N_3^- and either ZnCPD·L-Phe or ZnCPD below 8 Å^{-1} in k space. Above 8 Å^{-1} the variation in the individual scans indicate that the noise has become significant (data not shown). The isolated $\chi(k)$ function of ZnCPD·L-Phe is very similar to that of ZnCPD, suggesting that in this region little structural change occurs for the binary complex. On the other hand, there are spectral differences between ZnCPD·L-Phe·N_3^- and ZnCPD, indicating that the structure of the ternary complex differs from that of the free enzyme.

DISCUSSION

The first coordination sphere of Zn in the solution state of ZnCPD consists of two distributions of atoms, with four atoms (N or O) located at an average distance of 2.024 ± 0.006 Å, and one atom (N or O) located at 2.54 ± 0.05 Å (Table 1; Zhang et al., 1992). The four-atom distribution remains the same for ZnCPD in its crystalline state, but the fifth atom is found at 2.36 ± 0.04 Å, indicating that a change in the metal coordination sphere occurs upon crystallization. Examination of the higher coordination shell, between 2.7 and 4.2 Å, reveals the presence of two imidazoles. Combined with X-ray crystallographic results, the four atoms at an average distance of 2.024 Å are assigned to the two δ_1 nitrogens of His-69 and His-196, one ϵ_1 oxygen of Glu-72, and the oxygen of a coordinated water molecule (Zhang et al., 1992). The atom at 2.54 Å for ZnCPD in solution is assigned to the ϵ_2 oxygen of Glu-72. The results for CoCPD are quite similar, with the four atoms at an average distance of 2.08 ± 0.01 Å and one atom at 2.50 ± 0.04 Å, which moves to 2.34 ± 0.04 Å in the crystalline enzyme. Thus, the XAFS studies show that the metal coordination spheres in the zinc and cobalt enzymes are quite similar in the solution state but differ from their crystalline counterparts.

L-Phe, the C-terminal product of the most rapidly turned-over peptide substrates of carboxypeptidase A, does not perturb the metal coordination sphere of ZnCPD markedly at pH 7 (Figure 1, Table 1), indicating that neither its amino group nor its carboxylate group likely bonds directly to the metal. This is further supported by the data analysis between 2.8 and 4.0 Å in the Fourier transform (Figures 3 and 5). The similarity of the $\chi(k)$ functions of ZnCPD·L-Phe and ZnCPD suggest that the structure in this region is not perturbed by a bulky group such as the benzyl group of L-Phe. However determination of the expected amplitude change for addition of only a few atoms in this region is difficult, in particular when the spatial distribution of the atoms is broad. Thus the presence of an amino or carboxyl group of L-Phe might account for the small differences observed between ZnCPD·L-Phe and ZnCPD in the 2.8 to 4.0 Å transform (Figure 5).

The results of ^{13}C NMR T_1 and T_2 measurements of carboxylate-^{13}C enriched L-Phe binding to the cobalt enzyme (Luchinat et al., 1988) are consistent with the XAFS structure of the ZnCPD·L-Phe complex. The distance measurement calculated for the Co to ^{13}C carboxylate from T_{1p}^{-1} is 3.9 Å, indicating the carboxylate does not bind to the metal. In addition, the visible absorption spectrum of CoCPD is not markedly perturbed by the binding of L-Phe at neutral pH values (Latt & Vallee, 1971) again consistent with L-Phe not binding directly to the metal. In contrast to carbonic anhydrase (Lindskog, 1963) and horse liver alcohol dehydrogenase (Maret & Zeppezauer, 1986), binding of anions to carboxypeptidase A is extremely weak at neutrality as reflected in the relative insensitivity of the cobalt visible absorption spectrum of CoCPD to anions (Latt & Vallee, 1971). However, chemical modification of the Glu-270 residue of carboxypeptidase A gives rise to anion sensitivity at pH 7, leading to the proposal that the metal-coordinated water is stabilized by a hydrogen bond to the deprotonated Glu-270 at neutrality (Geoghegan et al., 1983; Figure 6, EH species). The fact that anions also markedly perturb the cobalt absorption spectrum in the presence of L-Phe led to

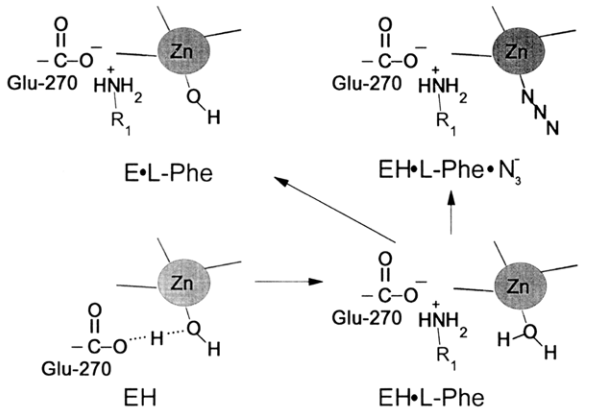

FIGURE 6: Schematic of different active site forms of carboxypeptidase A.

Table 2: Spectral Properties of Inhibitor Complexes of CoCPD

enzyme complex	electronic absorption λ_{max}, nm (ϵ, M^{-1}, cm^{-1})	^{1}H NMR[a] chemical shift (ppm) a	c	d	b
CoCPD	555 (150) 572 (150[b]	62	52	45	56
CoCPD•L-Phe	555 (200) 574 (205)[b]	61	52	47	58
CoCPD•L-Phe•N_3^-	308 (1250) 590 (330)[c]	61	55	45	73

[a] Isotopically shifted signals from protons of residues ligated to the cobalt (Bertini et al., 1988). [b] Data of Latt and Vallee (1970). [c] Data from Bicknell et al. (1988).

the proposal that the amino acids also disrupt the metal−H_2O−Glu-270 interaction (Bicknell et al., 1988; Bertini et al., 1990; Figure 6, EH•L-Phe species).

The XAFS results indicate that the addition of azide to the ZnCPD•L-Phe and CoCPD•L-Phe complexes markedly changes their metal coordination spheres (Figures 2−4). Only one distribution of four N/O atoms is now found for both enzymes (Table 1). The average interatomic distance for the zinc and cobalt ternary complexes decreases by about 0.03 Å when compared to the free enzymes. This corresponds to 0.12 Å for one ligand if the bond distance for other three is unchanged. The decrease in distance likely reflects the ligand exchange from a neutral water molecule to a charged anion. Examination of the higher coordination shell between 2.8 and 4.0 Å reveals marked changes that occur when azide is bound, providing further support for this assignment (Figures 3 and 5). This is the region where the second and third nitrogens of a zinc-bound azide would be expected to reside. Both single and multiple scattering paths of these nitrogens can lead to a focusing effect that can account for the observed spectral changes. Ultraviolet/visible spectroscopic studies of CoCPD also indicate that azide binds to the cobalt atom. The electronic absorption spectrum of CoCPD•L-Phe•N_3^- has a band at 308 nm characteristic of a charge transfer complex, and a new λ_{max} at 590 nm with a markedly elevated extinction coefficient, 330 M^{-1} cm^{-1} (Table 2; Bicknell et al., 1988).

The XAFS studies show the metal ligand at 2.5 Å has been displaced farther away in the ternary azide complexes of the zinc and cobalt enzymes. This change in coordination properties may reflect an alteration in the Glu-72 γ-carboxylate position from bidentate to monodentate ligation. ^{1}H NMR spectroscopy of the isotropically shifted signals in CoCPD, CoCPD•L-Phe, and CoCPD•L-Phe•N_3^- are also consistent with the XAFS observations (Bertini et al., 1988; Auld et al., 1992). The isotropically shifted signals a, c, and d of CoCPD were assigned to the NH-proton of His-69 and to the C-4 protons of His-69 and His-196, respectively. These signals are shifted no more than 2 ppm in the CoCPD•L-Phe complex (Table 2), in agreement with the close similarity of the XAFS spectra of the corresponding zinc complexes in their back-transformed 2.8−4.0 Å spectra (Figure 5). In addition a fourth signal, b, observed in the NMR was tentatively assigned to the γ-CH_2 protons of the Glu-72 ligand. This signal shifted only 2 ppm in the CoCPD•L-Phe complex but shifted 17 ppm in the CoCPD•L-Phe•N_3^- complex (Table 2). The XAFS results on the cobalt and zinc enzymes indicate this assignment is likely correct since the position of the second oxygen of the Glu-72 ligand is not greatly changed in the L-Phe complexes but is shifted markedly in the enzyme•L-Phe•azide complex (Figures 2−4, Table 2).

The XAFS results thus indicate that N_3^- displaces the water molecule and moves the second oxygen of Glu-72 farther away. The interaction of the protonated α-amino group of L-Phe with the ionized form of Glu-270 likely allows the displacement of the metal-bound water by N_3^- (Figure 6). X-ray crystallographic attempts to determine the structure of this ternary complex are very difficult to interpret because of severe cracking of the crystals even when they are crosslinked with glutaraldehyde (Mangani & Orioli, 1992). The results are consistent, however, with a model in which the azide ion binds to the metal.

The lack of effect of pH on the XAFS spectrum of the ZnCPD•L-Phe•N_3^- complex is also consistent with the metal-bound water being displaced by azide. Since the ionizable water is no longer present in the ternary complex, the XAFS spectrum is insensitive to changes in pH (Figure 4B).

Inhibition studies show that L-Phe shifts pK_{EH} from 9 to 7.5 at 25 °C (Auld & Vallee, 1987). In addition ^{1}H NMR spectroscopy studies of CoCPD indicate that L-Phe binding shifts the spectral pK_a of 8.84 observed for the free enzyme to 7.73 (Auld et al., 1992). The results of the XAFS studies of the ZnCPD•L-Phe complex are consistent with a downward shift in pK_{EH} (Figures 1 and 4, Table 1). Both the zinc enzyme (Zhang & Auld, 1993) and its L-Phe complex show a progressive decrease in their average ligand−metal distances as pH is increased (Table 1). However the alkaline XAFS spectrum for the L-Phe complex is now fully formed by pH 8.83 at 25 °C one whole pH unit below that observed for the native enzyme (Figures 1 and 4). The predominant form of L-Phe over the pH range 6.5 to 9 contains the protonated α-amino group due to its pK_a of 9.3. Thus, the most likely reason for the decrease in pK_{EH} for the L-Phe complex is that the protonated form of L-Phe binds more tightly to E than to EH. The protonated α-amino group of L-Phe forms an ionic bridge to the carboxylate of Glu-270, thus disrupting the hydrogen bond between the carboxylate and the metal-bound water molecule (Figure 6). The no longer H-bonded water ligand is now free to ionize at a lower pH value and, in addition, can be displaced by anions. In fact, the ternary ZnCPD•L-Phe•N_3^- complex likely mimics the one expected to be present after cleavage of the peptide bond. In that case the N-terminal product carboxylate would be the anion bound to the zinc.

While no X-ray crystallographic results have been reported for the L-Phe complex, they have been reported for the D-Phe

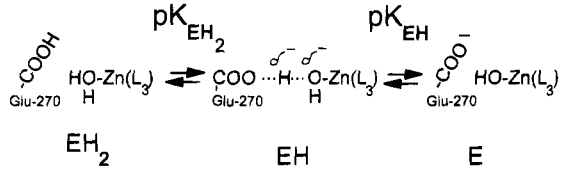

FIGURE 7: Schematic of ionizable groups critical to carboxypeptidase A catalysis.

complex (Christianson et al., 1989). In this case the α-amino group of D-Phe H-bonds to the carboxylate of Glu-270, which no longer interacts with the metal-bound water. Similar interactions for L-Phe might therefore be anticipated.

For several reasons pK_{EH_2} has been assigned to the ionization of the carboxyl group of Glu-270 and its accompanying interaction with the zinc-bound water, stabilizing the active-site structure ($EH_2 \rightleftarrows EH$, Figure 7). The crystallographic zinc−carboxylate interatomic distance is 4.5 Å, consistent with an intervening H-bonded water molecule (Lipscomb, 1973). Chemical modification of Glu-270 with CMC inactivates the enzyme (Riordan & Hayashida, 1973; Nau & Riordan, 1975). Temperature-jump studies provide evidence for a conformational change coupled to the formation of the EH_2 form of the enzyme which might reflect movement of Glu-270 away from the metal (French et al., 1974). The present XAFS studies of Zn and CoCPD in conjunction with previous spectrokinetic and NMR studies on CoCPD show that the binding of anions to the EH_2 form is reasonable since protonation of Glu-270 breaks its interaction with the water, allowing it to be displaced (Geoghegan et al., 1983; Bicknell et al., 1988; Auld et al., 1992; Figure 6). On the other hand the enzyme is inhibited by zinc hydroxide, which binds to the EH form of the enzyme (Larsen & Auld, 1989, 1991). This is also consistent with this model since the positive $ZnOH^+$ can bind to the negative Glu carboxylate oxygen and displace the metal bound water forming a Zn−O−Zn bridge.

The zinc bound water therefore functions in both the acid and alkaline pK_a values of carboxypeptidase A. It needs to be in its protonated state ($[ZnL_3(H_2O)]^+$) to be catalytically active. In this way it can poise the ionized carboxylate Glu-270 for catalysis (Vallee and Auld, 1990b, 1993). Ionization of the water at alkaline pH values decreases the charge on the zinc, making it a poorer Lewis acid for interaction with the substrate. This in turn leads to a weaker interaction with the substrate as is observed in catalysis (Auld & Vallee, 1970, 1971, 1987).

ACKNOWLEDGMENT

We appreciate the support of the staff of the NBPRT beamline X9-B and the National Sychrotron Light Source. The NBPRT is supported by NIH Research Resource Grant RR-01633.

REFERENCES

Auld, D. S. (1988) *Methods Enzymol. 158*, 71−79.
Auld, D. S., & Vallee, B. L. (1970) *Biochemistry 9*, 4352−4359.
Auld, D. S., & Vallee, B. L. (1971) *Biochemistry 10*, 2892−2897.
Auld, D. S., & Vallee, B. L. (1987) Carboxypeptidase A, in *Hydrolytic Enzymes* (Neuberger, A., & Brocklehurst, K., Eds.) pp 201−255, Elsevier, New York.
Auld, D. S., & Zhang, K. (1995) *FASEB J. 9*, A1326.
Auld, D. S., Bertini, I., Donaire, A., Messori, L., & Moratal, J. M. (1992) *Biochemistry 31*, 3840−3846.
Bertini, I., Luchinat, C., Monnanni, R., Moratal, J. M., Donaire, A., & Auld, D. S. (1990) *J. Inorg. Biochem. 39*, 9−16.
Bicknell, R., Schaffer, A., Bertini, I., Luchinat, C., Vallee, B. L., & Auld, D. S., (1988) *Biochemistry 27*, 1050−1056.
Bunker, G., Stern, E. A., Blankenship, R. E., & Parson, W. W. (1982) *Biophys. J. 37*, 539−551.
Christianson, D. W., Mangani, S., Shoham, G., & Lipscomb, W. N. (1989) *J. Biol. Chem. 264*, 12849−12853.
Crozier, E. D., Rehr, J. J., & Ingalls, R. R. (1988) in *X-ray Absorption: Principle, Application, Techniques of EXAFS, SEXAFS, and XANES* (Koningsberger, D. C., & Prins, R., Eds.) pp 373, John Wiley and Sons, New York.
French, T. C., Yu, N.-T., & Auld, D. S. (1974) *Biochemistry 13*, 2877−2882.
Geogehegan, K. F., Holmquist, B., Spilburg, C. A., & Vallee, B. L. (1983) *Biochemistry 22*, 1847−1852.
Holmquist, B. (1988) *Methods Enzymol. 158*, 6−12.
Horrocks, W. DeW., Jr., Ishely, J. N., Holmquist, B., & Thompson, J. S. (1980) *J. Inorg. Chem. 12*, 131−141.
Larsen, K. S., & Auld, D. S. (1989) *Biochemistry 28*, 9620−9625.
Larsen, K. S., & Auld, D. S. (1991) *Biochemistry 30*, 2614−2618.
Latt, S. A., & Vallee, B. L. (1971) *Biochemistry 10*, 4263−4269.
Lee, P. A., Citrin, P. H., Eisenberger, P., & Kincaid, B. M. (1981) *Rev. Mod. Phys. 53*, 769.
Lindskog, S. (1963) *J. Biol. Chem. 238*, 945−951.
Lipscomb, W. N. (1973) *Proc. Natl. Acad. Sci. U.S.A. 70*, 3797−3801.
Luchinat, C., Monnanni, R., Roelens, S., Vallee, B. L., & Auld, D. S. (1988) *Inorg. Biochem. 32*, 1−6.
Mangani, S., & Orioli, P. (1992) *Inorg. Chem. 31*, 365−368.
Maret, W., & Zeppezauer, M. (1986) *Biochemistry 25*, 1584−1588.
Nau, H., & Riordan, J. R. (1975) *Biochemistry 14*, 5285−5294.
Rees, D. C., Lewis, M., & Lipscomb, W. N. (1983) *J. Mol. Biol. 168*, 367−387.
Riordan, J. F., & Hayashida, H. (1970) *Biochem. Biophys. Res. Commun. 41*, 122−127.
Stern, E. A., & Heald, S. M. (1983) in *Handbook of Synchrotron Radiation* (Koch, E. E., Ed.) pp 955−1014, North-Holland, New York.
Stern, E. A., Ma, Y., Hansk-Petitpierre, O., & Bouldin, C. E. (1992) *Phys. Rev. B 46*, 687.
Vallee, B. L., & Auld, D. S. (1990a) *Biochemistry 29*, 5647−5659.
Vallee, B. L., & Auld, D. S. (1990b) *Proc. Natl. Acad. Sci. U.S.A. 87*, 220−224.
Vallee, B. L., & Auld, D. S. (1993) *Acc. Chem. Res. 26*, 543−551.
Zhang, K., & Auld, D. S. (1993) *Biochemistry 32*, 13844−13851.
Zhang, K., Stern, E. A., Ellis, F., Sanders-Loehr, J., & Shiemke, A. K. (1988) *Biochemistry 27*, 7470−7475.
Zhang, K., Chance, B., Auld, D. S., Larsen, K. S., & Vallee, B. L. (1992) *Biochemistry 31*, 1159−1168.
Zhang, K., Rosenbaum, G., & Bunker, G. (1993) *Jpn. J. Appl. Phys., Part 2 32*, 147−149.
Zhang, K., Dong, J., & Auld, D. S. (1995) *Phys. B 208/209*, 719−721.

BI951816T